1 # Quantifying the impacts of wildfires on soil thermal, hydrological
2 # and carbon dynamics in northern Eurasia from 2003 to 2016

3 Yiming Xu[1], Qianlai Zhuang[1], Bailu Zhao[1], Michael Billmire[2], Christopher Cook[2], Jeremy
4 Graham[2], Nancy HF French[2], Ronald Prinn[3]

5 [1] Department of Earth, Atmospheric and Planetary Sciences, Purdue University, West Lafayette, IN 47907 USA
6 [2] Michigan Tech Research Institute, Michigan Technological University, Ann Arbor, MI 48105 USA
7 [3] Department of Earth, Atmospheric, and Planetary Sciences, MIT, Cambridge MA

8

9 *Correspondence to*: Qianlai Zhuang (qzhuang@purdue.edu)

10 To be submitted to Biogeoscience

11 **Abstract.** We use a process-based biogeochemistry model to simulate the fire impacts on soil thermal and hydrological

12 dynamics and carbon budget of forest ecosystems in Northern Eurasia during 2003-2016 based on satellite-derived

13 burn severity data. We find that burn severity generally increases in this region during the study period. Simulations

14 indicate that fires increase soil temperature by 0.2-0.5 $^\circ$C through removing the ground moss and surface soil organic

15 matter, especially in Asian part of the region. Fires also increase water runoff by about 131 million m^3 yr^{-1} through

16 reducing post-fire evapotranspiration, leading to a higher regional river discharge. Fires remove 1.7 Pg C of ecosystem

17 carbon through combustion emissions during this period and reduce net ecosystem production from 106.4 to 66.1 Tg

18 C yr^{-1}. Fires lead the forest ecosystems to lose 2.3 Pg C, shifting the forests from a carbon sink to a source in this

19 period. Our study highlights the importance of wildfires in affecting soil thermal and hydrological and carbon

20 dynamics in boreal forests.

21

22 1 Introduction

23 Boreal forests store more than one-third of the global terrestrial carbon, playing an important role in the global carbon

24 cycling (Kasischke & Stocks., 2000). This large carbon pool is vulnerable to wildfire disturbance (Helbig et al., 2016).

25 Fire can release large amounts of carbon into the atmosphere through direct combustion emission and decrease post-

26 fire ecosystem production (Kurz & Apps, 1999; Amiro et al., 2006; Yin et al., 2020; Zhao et al., 2021), thereby

27 increasing carbon dioxide concentration in the atmosphere. Recent studies show that burn area and burn severity are

28 increasing in boreal forests under the anthropogenic climate warming (Gillett et al., 2004; Zheng et al., 2021; Iglesias

29 et al., 2022), suggesting there are positive feedbacks between fires and the global climate (Moubarak et al., 2023).

30

31 Previous studies show that the river discharge in Eurasia high latitude regions has been increasing (Peterson et al.,

32 2002; McClelland et al., 2006; Overeem & Syvitski, 2016). This change might be due to permafrost thaw

33 (Lamontagne-Hallé et al., 2018; Wang et al., 2021) and wildfires. Wildfires can influence soil thermal and

34 hydrological regime. Specifically, wildfires change the soil hydrology of forests by removing vegetation canopy,

1   reducing evapotranspiration (Poon & Kinoshita, 2018). They can also enhance post-fire water runoff (Moody & Martin,

2   2001; Thomas et al., 2021) by changing vegetation and soil texture (Shakesby & Doerr, 2006; Moody et al., 2009;

3   Ebel & Martin., 2012). These dynamics are also affected by varying burn severities (Moody et al., 2008). Previous

4   studies show that fire can increase soil surface temperature through direct heat release (Franklin et al., 1997; Debano

5   et al., 1998, Certini, 2005) and influence the energy balance of soil surface (Li et al., 2017; Zhao et al., 2021) by

6   changing the albedo and evapotranspiration of the vegetation.

7

8   Wildfires impact the carbon cycle of boreal forests by removing aboveground vegetation and consuming soil organic

9   matter (Turquety et al., 2007; Turetsky et al. 2011, de Groot et al., 2013; Rogers et al., 2015). Soil organic matter

10   combustion can release large amounts of carbon into the atmosphere, accounting for up to 90% of the total carbon

11   emission for severe fires (Walker et al., 2018). In addition to direct combustion emissions, post-fire soil respiration

12   can also impact the carbon budget due to changing soil temperature and moisture (Kulmala et al., 2014). After fire,

13   there might also be a vegetation shift (Denslow, 1980; Gewehr et al., 2014; Stuenzi et al., 2022). With the change in

14   ecosystem structure, soil moisture and soil temperature, carbon dynamics can be significantly affected (Sullivan et al.,

15   2011; Li et al., 2017).

16

17   Previous studies have modeled fire's influence on soil physical properties and carbon dynamics with limitations. Many

18   of them mainly focus on direct combustion emissions (Conard & Ivanova, 1997; Amiro et al., 2001; French et al.,

19   2002). Some studies are on site level and lack regional quantification (Moody qt., 2008; Van Eck et al., 2016; Poon

20   & Kinoshita, 2018). Further, existing studies typically have not incorporated the effects of burn severity because its

21   data are unavailable or difficult to obtain (Kasischke et al., 2005; Balshi et al., 2007; Van Eck et al., 2016). Some

22   studies have tried to overcome these limitations by using process-based models (Zhao et al., 2021), but have not

23   focused on analyzing soil hydrological regime, especially in Eurasia high latitudes. These modeling studies could be

24   improved by using burn severity information to holistically understand how fires affect soil thermal and hydrological

25   and carbon dynamics.

26

27   In this study, we use a sophisticated process-based model, the Terrestrial Ecosystem Model (TEM) (Zhuang et al.,

28   2002; Zhao et al., 2020; Xu et al., 2024) to quantify the influence of fire on regional soil thermal, hydrological, and

29   carbon dynamics in Eurasia northern high latitude forests. With satellite-derived burn severity data, we analyze these

30   impacts from 2003 to 2016.

31

32   **2 Data and method**

33   **2.1 Burn severity data**

34   Fire burn area perimeters were obtained from the Global Fire Atlas (Andela et al, 2019), which were derived from

35   MODIS daily moderate-resolution (500 m) Collection 6 MCD64A1 burned-area data from 2003 (the start of the

1   MODIS mission) to 2016. To reduce the Global Fire Atlas down to the areas of interest, annual detected burn area

2   shapefiles were first input to the QGIS Repair Geometry tool to clean geometries, then clipped to the extents of Europe

3   and Asia north of 45 degrees, for each year of 2003-2016. Batch processing capabilities available within QGIS were

4   then used to reproject shapefiles to Asia/Europe Albers Equal Area Conic and remove all fire shapefiles of less than

5   2 hectares. Overlapping fire detections within a single year were combined using QGIS 'Dissolve' and allowed for

6   keeping of associated polygon information.

7

8   Because the Global Fire Atlas is based on MODIS fire detections, the available fire shapefiles had an inherent

9   blockiness and holes within fire perimeters. The geometry was simplified by reducing the number of vertices but

10   thresholding to not change any features by more than 250 meters, the native resolution of the burned area product.

11   Interior holes within the perimeters were filled in to further simplify the geometry. This allowed for more feasible

12   processing times for subsequent buffering operations. Many of these holes were water bodies where values would be

13   removed from the analysis by optical cloud masking. In the cases where the holes were not water, it was considered

14   that they could either be real unburned areas within the perimeter, or false negatives that actually burned but not hot

15   enough to trigger the active hotspot detection. However, it was determined that these scenarios would balance out at

16   the scale of the analysis.

17

18   A Google Earth Engine (GEE) script was developed to calculate a pre- and post- Normalized Burn Ratio (NBR) value

19   from within each FIRE perimeter, as well as from within a 300 m buffer ring offset 1.5 km from the perimeter. Data

20   were sourced from Landsat 4-8 collections and used median pixel values after applying a cloud, cloud shadow, snow,

21   and water mask. NBR for each fire was calculated as the ratio between the near infrared (NIR) and short-wave infrared

22   (SWIR) bands for the available Landsat mission:

23   $NBR = \dfrac{NIR - SWIR}{NIR + SWIR}$ (1)

24   Pre-fire data use the median pixel values of the image collection, with images filtered to the approximate snow-free

25   fire season of June 15 to September 15, from the two years before the fire. Post-fire data use the median pixel values

26   from the image collection June 15 to September 15 the year following the fire. The median pixel values from within

27   the perimeter and buffer ring averaged to create a pre-fire NBR and post-fire NBR for each perimeter and buffer ring.

28   These NBR values were written out of GEE along with each unique fire ID. Methods in the GEE code for masking

29   and pooling the Landsat 4-8 data were sourced from Holsinger et al. (2021).

30

31   The values in the buffer ring are used to correct differences between the imagery not related to the fire (e.g., phenology,

32   plant health), as this land area is assumed to have not burned. One caveat is that in some areas that had nearby fires

33   within the same year, there may be some overlap between the buffer ring and another fire perimeter, however these

34   cases are uncommon. The difference between the pre-fire NBR - the postfire NBR is known as the delta NBR (dNBR)

35   and can be used to estimate burn severity for a fire:

36   $dNBR = NBR_{prefire} - NBR_{postfire}$ (2)

1 In addition to calculating dNBR for each individual fire over 2003-2016, data were aggregated at a 0.5°×0.5° grid cell

2 for each year in order to incorporate these data into modeling.

3

4 **2.2 Model description**

5 We use the Terrestrial Ecosystem Model (TEM; Zhuang et al., 2002) that simulates soil thermal, hydrological regime

6 and carbon dynamics in terrestrial ecosystems. TEM has been used to simulate fire disturbance on carbon dynamics

7 and soil thermal regime in North America (Zhuang et al., 2002; Zhao et al., 2021; Xu et al., 2024). Apart from direct

8 carbon emission due to combustion, TEM can also simulate post-fire carbon dynamics during the ecosystem recovery

9 (Fig. 1; Zhao et al., 2021; Xu et al., 2024).
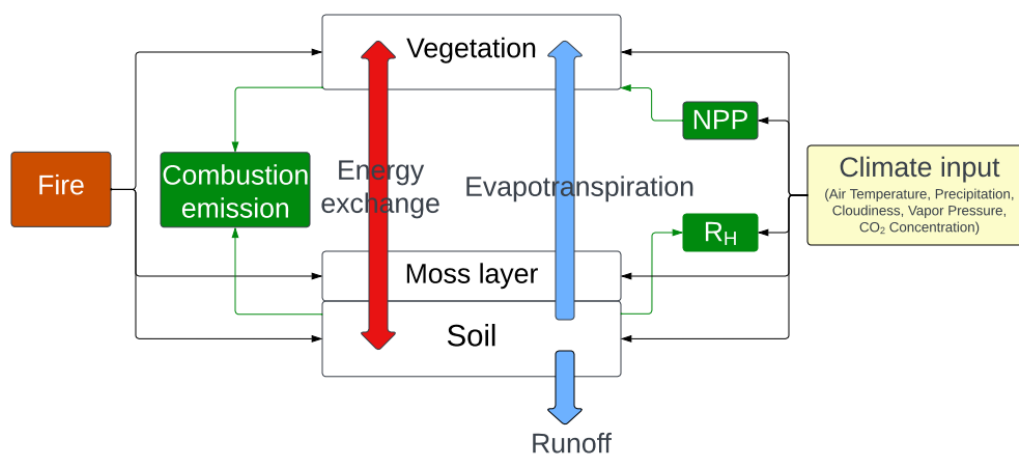
10
11 **Figure 1: Fire effects on forest ecosystem dynamics of energy, water, and carbon.**

12

13 The calculated delta Normalized Burn Ratio (dNBR) values that represent burn severity for fires are used to estimate

14 the proportion of vegetation and soil carbon consumption in TEM (Zhuang et al., 2002; Zhao et al., 2021). In the

15 model, fire removes carbon from vegetation and soil based on the burn severity. First, TEM estimates the composite

16 burn index (CBI) based on dNBR values:

17 $CBI = p_1 \times dNBR + p_2$ (3)

18 where P_1 and P_2 are parameters calibrated in the previous study (Zhao et al., 2021). With estimated CBI value, the

19 removed carbon is calculated based on:

20 $R = p_3 \times CBI + p_4$ (4)

21 where R is the removed ratio, P_3 and P_4 are parameters given by field measurement (Boby et al., 2010).

22

1   Fires with greater burn severity remove more carbon from the ecosystem. Following fire, the reduction in litter-fall

2   might further impact soil organic carbon composition during the vegetation recovery. The reduced vegetation carbon

3   storage can result in lower ecosystem production during the recovery phase.

4

5   Fire also impacts soil temperature and soil water content. In TEM, soil thermal regime is simulated with surface air

6   temperature and land surface energy exchange process that is influenced by the canopy and moss (Xu et al., 2024).

7   Simulated vegetation canopy and ground moss layer can impact soil physical properties. Fire removes ground moss

8   layer which serves as an insulation in the soil thermal module. In the year of fire, TEM assumes that the fire completely

9   combusts the moss. After fire, the moss thickness recovers as the following:

10     $moss = a_1 \times (1 - e^{b_1 \times t})$ (5)

11   where moss is the moss thickness (cm), t is the year after fire, a_1 and b_1 are parameters. Also, canopy can influence

12   the surface energy budget and soil surface temperature. The soil surface energy budget is estimated as:

13     $Q = SH + LH + SR + LR$ (6)

14   where Q is the energy budget, SH is the sensible heat flux, LH is the latent heat flux, SR is the short-wave radiation

15   and LR is the long-wave radiation. These variables are calculated based on the meteorological input data and leaf area

16   index. More details can be found in Xu & Zhuang (2023). The removal of ground vegetation by fire will change the

17   soil energy exchange and impact the soil temperature. On the other hand, soil temperature and soil moisture will affect

18   the growth of the vegetation. These influences on soil physical properties can further change carbon dynamics, such

19   as heterotrophic respiration (R_H), since these processes are highly correlated with soil thermal regime.

20   Soil water content and runoff are estimated with precipitation, evaporation and the soil texture. Fire-derived changes

21   of vegetation will affect the evaporation process and in turn impact the soil hydrological regime. In TEM, transpiration

22   is calculated as (Zhuang et al., 2002):

23     $trans = \dfrac{slope \times drad + c_p \times pa \times \frac{vpd}{ra}}{(slope + gamma \times (1 + \frac{rc}{ra})) \times le} \times dayl$ (7)

24   where *trans* is transpiration (mm/month), slope is the slope of vapor pressure curve, *drad* is the canopy daily average

25   radiation, a function of the leaf area index. C_p is the specific heat of air (J kg^{-1}K^{-1}), *pa* is the density of air (kg m^{-3}),

26   *vpd* is the vapor pressure deficient from canopy to air (mbar), *ra* is canopy aerodynamic resistance, *rc* is canopy

27   resistance to water vapor, *le* is latent heat of vaporization of water (J kg^{-1}), *dayl* is the length of a day (s) and *gamma*

28   is a parameter. The water exceeding the soil capacity is calculated as runoff. In the model, fire removes ground

29   vegetation, the amount of removal depends on the burn severity. The reduced leaf area index leads to lower

30   evapotranspiration and higher soil water content, resulting in higher runoff.

31   **2.3 Input data and simulation protocols**

32   Monthly mean surface air temperature, cloudiness, precipitation, vapor pressure, and surface wind speed from ERA5

33   (Hersbach et al., 2020) during 2003-2016 are used to drive the model. Spatially-explicit soil texture (percentage of

34   silt, clay and sand), elevation, plant function types and annual CO_2 concentrations of the atmosphere are also used

35   (Melillo et al., 1993; Zhuang et al., 2002).

1   The model is calibrated in previously published work (Zhuang et al., 2002; Zhao et al., 2021). It can well estimate the

2   soil and vegetation carbon in three Canadian boreal sites (Zhao et al., 2021). The parameters used in this study are

3   adopted from this previous work.

4

5   The model is spun-up for 120 years before 2003 with cyclic climate data from 1988 to 2003 to achieve an equilibrium

6   state. Then transient simulations from 2003 to 2016 are conducted for each grid cell at a spatial resolution of $0.5°×0.5°$

7   for the Eurasia high latitude forests.

8

9   We conduct two regional simulations, with and without fire disturbance considered, respectively. Fire polygons are

10 dissected into each unit with unique fire history and then intersected with each grid cell when considering fire impacts.

11 The output values for each grid cell are area-weighted mean of each fire polygon and no-burn area within the cell

12 (Zhao et al., 2021). To test the sensitivity of the four parameters in equations 1 and 2, we also conduct four additional

13 simulations with modifications of the parameters. In each simulation, we increase one parameter by 10% and compare

14 the results with original simulations.

15

16 **3 Results**

17 **3.1 Changes in fire regime**
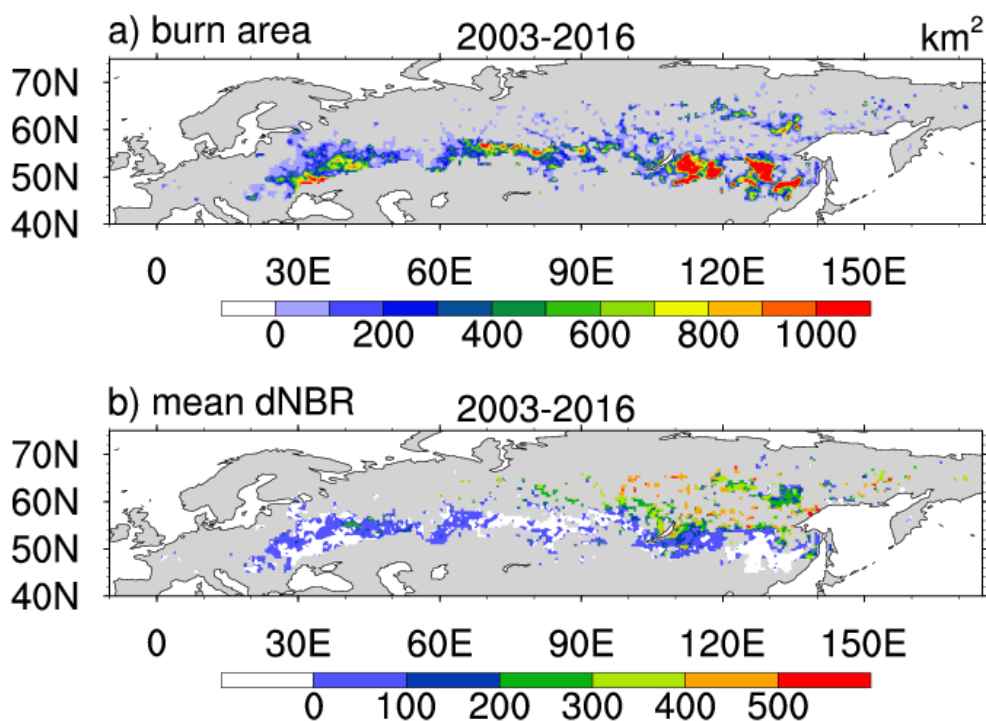
18

1 **Figure 2: Burn area (a) (units: km2) and severity (b) (delta Normalized Burn Ratio, dNBR values) in Eurasia forests during**
2 **2003-2016.**

3 Most grid cells are burned for less than 300 km^2 during 2003-2016 while the maximum area can be larger than 1000

4 km^2 for East Europe, Central Asia and Northeast Asia (Fig. 2). For the burn severity, the mean dNBR value is less

5 than 150 for most grid cells while it can be greater than 350 for most grids in East Russia. For those widely-burned

6 grid cells (Fig. 2a), the burn severities are generally low, with widely-spread dNBR values that are smaller than 0 (Fig.

7 2b). This means that high severity fires mostly occur in a small area, and mild fires take up more land during the study

8 period (Fig. 3a). There is a significant increasing trend of the regional mean burn severities from 2003 to 2016 (Fig.

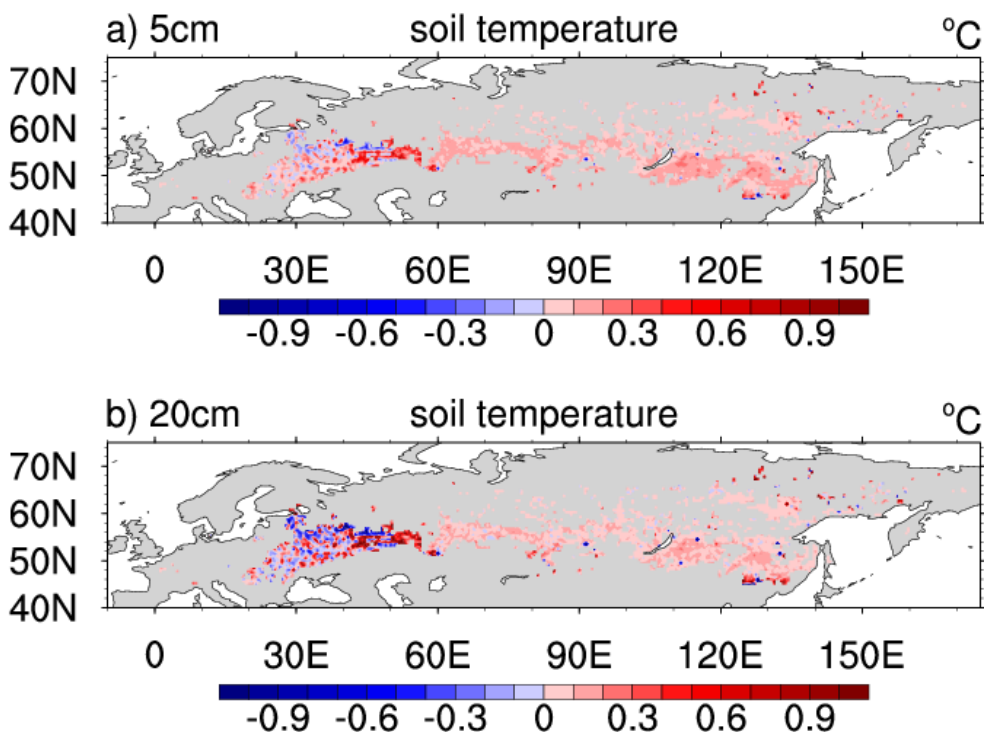**9** 3b) with a slope of 4.9 and a P value of 0.038.

10
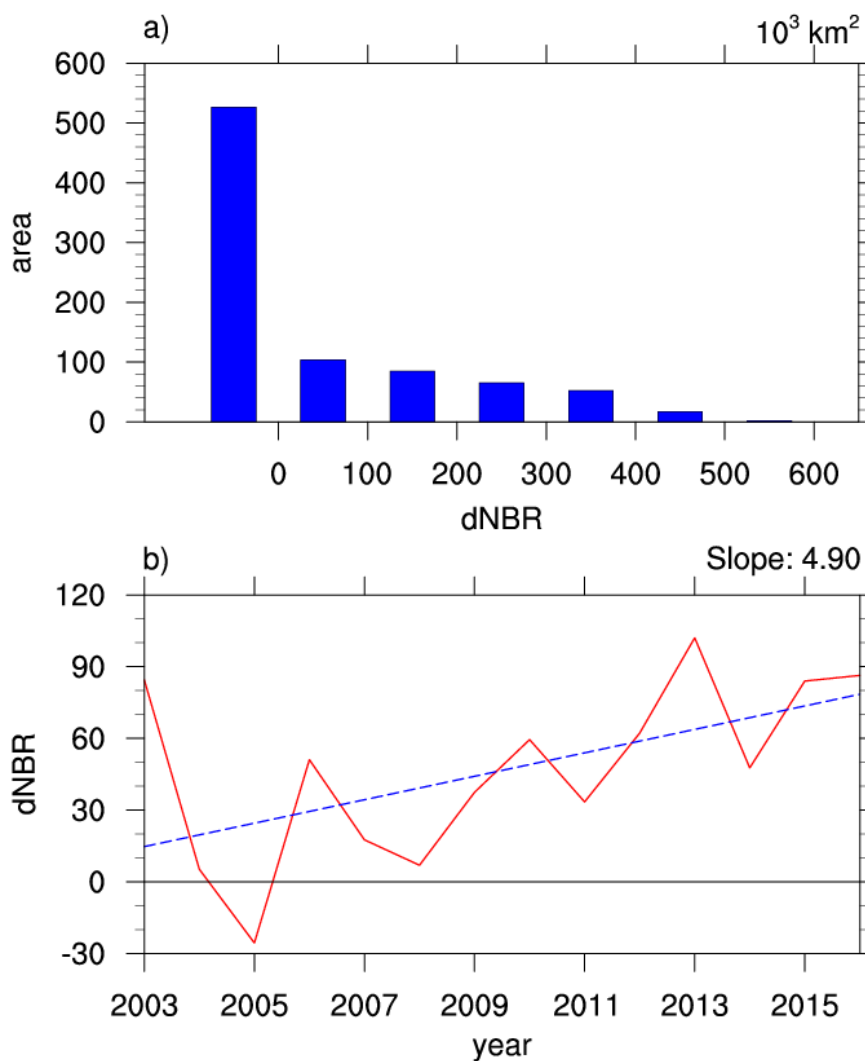
11

Figure 3: Summary of fire regimes: (a) Histograms of dNBR. The heights of bars are total fire area in which average dNBR is within the thresholds indicated by the x axis. (b) Annual area-weighted mean dNBR value (red line) and its linear trend (blue line).

3.2 Fire impacts on soil thermal and hydrological regime


Figure 4: Simulated mean soil temperature differences with fire minus without fire in Eurasia for 5 cm (a) and 20 cm (b) depth during 2003-2016.

Compared with no fire simulation, the model estimates higher mean soil temperature (Fig. 4) in Asia with a magnitude of 0.2-0.5 °C since fire can remove the ground moss layer which can insulate heat and cool the soil. The deep soil layer temperature change follows the pattern of the surface soil but exhibits smaller magnitudes. There is no clear pattern for soil temperature changes in Europe, especially for the 20 cm depth, since it is relatively warmer in Europe and the model estimates little or no ground moss layer in this area.
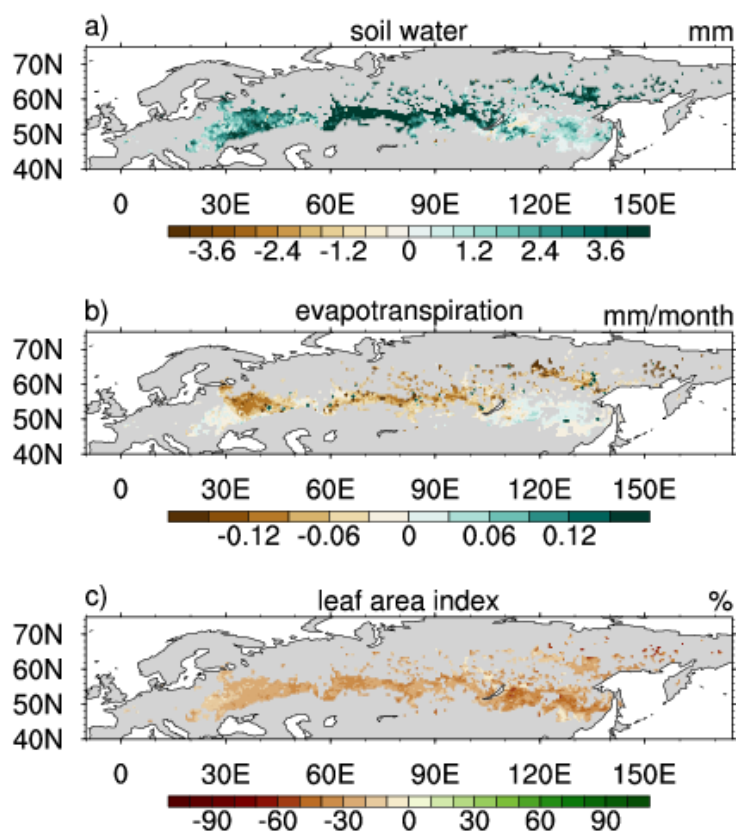
Figure 5: Simulated mean soil water content (a, for top 70cm soil), evapotranspiration (b) and relative leaf area index (c) differences due to fire (with fire minus without fire) during 2003-2016.

Due to fire, the simulated mean soil water content increases for most grid cells with a magnitude of more than 2 mm (Fig. 5a). The model also generally estimates lower evapotranspiration with a magnitude of 0.1 mm month-1 (Poon & Kinoshita, 2018). These changes can be attributed to the leaf area index change (Fig. 5c). After fire, simulated leaf area index decreases since fire significantly removes canopy and ground vegetation. Decreased leaf area index weakens evapotranspiration, leading to higher soil water content. As a result, the model estimates higher water runoff (Fig. 6) with a mean magnitude of around 131 million m^3 yr^{-1} for the whole region. The changes in water runoff due to fire show an increasing trend during 2003-2016, which is consistent with the annual mean burn severity trend (Fig. 3).

1
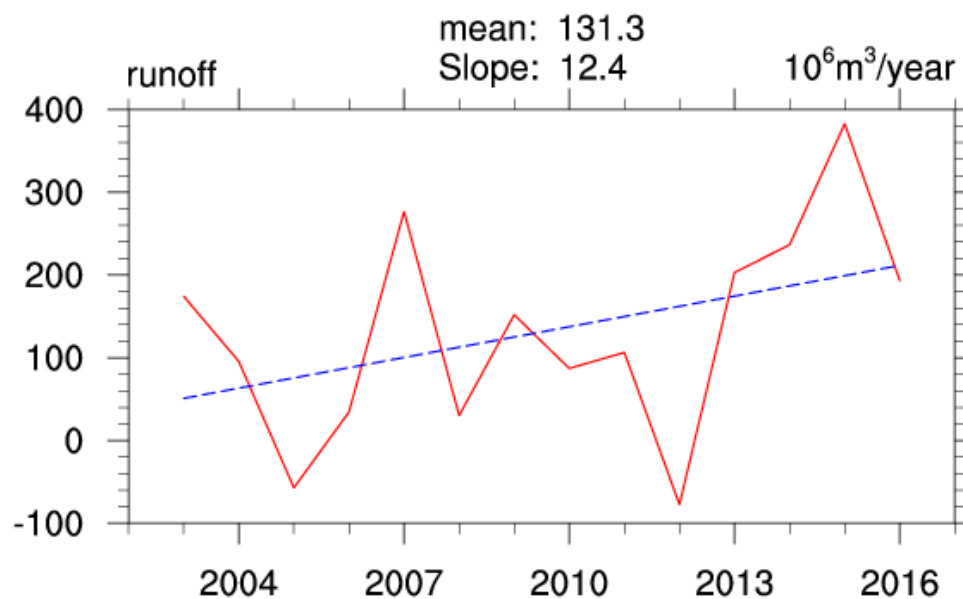
Figure 6: Temporal evolution of regional mean runoff differences (with fire minus without fire) in Eurasia.

3

4   **3.3 Fire impacts on carbon dynamics**

5   **Table 1: Regional mean NPP, RH, NEP and combustion emission in Eurasia during 2003-2016 for the two simulations.**

6

Units: Tg C yr^{-1}	Without fire	With fire
NPP	1177.5	1132.0
R_H	1071.0	1065.9
NEP	106.4	66.1
Combustion	/	121.9

7

8   When fire is not considered, the model estimates the whole region as a net carbon sink, with a mean net ecosystem

9   production (NEP) of 106.4 Tg C yr^{-1} (Table 1). When fire is considered, the simulated net primary production (NPP)

10   is lower since fire significantly removes vegetation carbon and decreases the gross primary production (GPP). Despite

11   higher soil temperature due to fire, the simulated heterotrophic respiration (R_H) decreases since fire removes soil

12   carbon. The magnitude of the changes in NPP is greater than R_H, leading to a decreased NEP. In all, the modeled NEP

13   is 66.1 Tg C yr^{-1} for the whole region, 40.3 Tg C yr^{-1} less than no fire situation. Although the model estimates a positive

14   regional NEP, the simulated regional combustion emissions of 121.9 Tg C yr^{-1} are much greater than NEP, resulting

15   in a net loss of carbon at 55.8 Tg C yr^{-1} during 2003-2016.

16

4 Discussion

4.1 Fire and river discharge

There is an increasing trend for both annual mean burn severity and water runoff during 2003-2016 in Eurasia. This might have increased river discharge (Peterson et al., 2002; Rood et al., 2017; Ahmed et al., 2020; Feng et al., 2021) to the Arctic Ocean and decrease the ocean salinity (Peterson et al., 2002; McPhee et al., 2009). Our simulated runoff differences due to fire in major river watersheds in Russia indicate that all watersheds exhibit an increase in the mean runoff due to fires (Table 2). Yenisei, Ob and Lena, the three major rivers that drain into the Arctic Ocean, exhibit relatively larger discharges than other rivers. Increasing river discharge and decreasing salinity might further influence the ocean circulation, such as Atlantic Meridional Overturning Circulation (AMOC) (Liu et al., 2019), impacting the global climate.

Table 2: Simulated mean runoff difference due to fire in 7 major river watersheds in Russia. (Units: million m3 yr-1).

Watersheds	Runoff Difference
Volga	3.7
Yenisei	16.4
Ob	36.1
Lena	7.8
Amur	0.8
Dnieper	0.03
Don	12.6

4.2 Comparison with other studies for carbon dynamics

We estimate that the total combustion emissions are 121.9 Tg C yr^{-1} for Eurasia high latitude forests during 2003-2016, which is slightly lower than that in previous studies focusing on Russia or Eurasia (Table 3). Our study only focuses on the forests in Eurasia high latitudes while these studies cover other vegetation types including tundra and grasslands for instance. Together with our previous estimates of fire emissions of 67.7 Tg C yr^{-1} from North America (Xu et al., 2024), we estimate the total combustion emissions from northern high latitude forests are 189.6 Tg C yr^{-1}. This is close to, but a little lower than previous estimates (Table 3).

Table 3: Combustion emission comparison with other studies (Units: Tg C yr-1).

Studies	Time	Region	Carbon emission
This study	2003-2016	Eurasia	121.9
Mouillot et al. (2006)	1990-1999	Eurasia	166
van der Werf et al. (2006)	1997-2004	Russia	188.4

Shvidenko et al. (2011)	1998-2010	Russia	82.0
Yue et al. (2016)	1997-2009	Pan-Arctic	200
Ponomarev et al. (2021)	2002-2020	Siberia	80±20
Zheng et al. (2023)	2000-2020	Eurasia	149.8*
Zheng et al. (2023)	2000-2020	Pan-Arctic	212.3*

1 *Calculated based on the global combustion emission flux data.

2

3 **4.3 Sensitivity and uncertainty analysis**

4 TEM estimates the proportion of carbon removal by using dNBR values to estimate the CBI and corresponding carbon

5 removal. The relationship between dNBR values and CBI (Eqn. 1) and the relationship between CBI and the

6 proportion of carbon removal (Eqn. 2) are based on field study (Zhao et al., 2021; Boby et al., 2010). Thus, those

7 parameters in the equations might have uncertainties. By raising each parameter by 10%, the estimated regional

8 combustion emissions all exhibit a slight increase (Table 4). The rising of P_3 leads to a most significant increase of

9 the combustion emission by 7.4%. This parameter is the slope of the linear regression relationship between CBI and

10 the proportion of removed carbon due to fire. Considering that equation 2 has a relatively low explained variance ratio

11 for the regression analysis, especially for canopy carbon (R^2=0.15, Boby et al., 2010), the relationship between CBI

12 and the combustion proportion leads to the largest uncertainty in our study.

13

14 **Table 4: Combustion emissions of sensitivity test simulations and their relative change compared with the original**

15 **simulation. The simulation name indicates the modified parameter in EqnS. 1 and 2.**

16

Simulation	Combustion emission (Tg C yr^{-1})	Percentage change (%)
P_1	126.6	3.9
P_2	125.8	3.2
P_3	131.0	7.4
P_4	124.7	2.3

17

18 Using dNBR values to represent burn severity in the model can also cause some uncertainties since other factors such

19 as moisture, elevation and time of burn can also impact burn severity (Kasischke & Hoy, 2012; Tan et al., 2007; Zhao

20 et al., 2021). The relationship between dNBR and combustion proportion is established for black spruce dominated

21 forests and the model is originally calibrated with field data from Alaska. This might induce uncertainties when

22 modeling Eurasia high latitude forests since the vegetation type and climate condition in Eurasia can be different from

23 Alaska. Additionally, we have not modeled the vegetation shift impacts after fire (Gewehr et al., 2014; Stuenzi et al.,

24 2022). Thus, the vegetation recovery after fire is not explicitly modeled, which might affect the corresponding soil

25 thermal and hydrological dynamics, in turn, influencing carbon dynamics.

1   **4.4 Limitations to this study**

2   First, in modeling fire impacts on hydrological dynamics, we assume that precipitation within a month occurs at one

3   event and the soil water that exceeds the soil water capacity is treated as runoff. This might overestimate the runoff

4   since it is highly possible that there is more than one precipitation event within a month. Second, the calculation of

5   evapotranspiration is based on the Penman-Monteith equation, but with some simplifications. Wind speed, used in the

6   equation, can influence the speed of evapotranspiration while TEM does not consider that. In addition, TEM only

7   considers the evapotranspiration in upper layers of the soil while deep layer soils might also impact this process if

8   roots can reach those layers. Third, TEM runs independently for each grid cell. There are no exchanges between

9   adjacent cells while water runoff is highly affected by the lateral water exchanges. Fourth, fire can affect post-fire

10   runoff through changing soil structure and texture (Shakesby & Doerr, 2006; Ebel & Martin., 2012), but this has not

11   been considered in the current model.

12

13   **5 Conclusions**

14   Driven with satellite-derived burn severity data, our model simulations show that increasing burn severity warms

15   regional mean soil surface temperature by 0.1-0.5 °C during 2003-2016 in Eurasia northern high latitude forests. Fires

16   decrease post-fire evapotranspiration and increase soil water content, leading to a higher runoff of 131 million m^3 yr^-

17   ^{1} in this region. Wildfires also significantly remove ecosystem carbon through combustion emissions of 121.9 Tg C

18   yr^{-1} and reduce post-fire ecosystem production from 106.4 to 66.1 Tg C yr^{-1}. As a result, wildfires cause those forests

19   to lose 2.3 Pg C during the study period, resulting in a shift from a carbon sink to a source. This study highlights the

20   importance of burn severity in modeling soil thermal, hydrological regime and regional carbon dynamics in northern

21   Eurasian forests.

22

23   **Conflict of interest**

24   The contact author has declared that none of the authors has any competing interests

25

26   **Acknowledgement**

28

29   **Open Research**

30   The data that support the findings of this study are openly available at the following:

31   Zhuang, Q. and Xu, Y.: Quantifying the impacts of wildfires on soil thermal, hydrological and carbon dynamics in

32   northern Eurasia from 2003 to 2016, doi: 10.4231/ZJM7-A207,2024

33

1   **References:**

2   Ahmed, R., Prowse, T., Dibike, Y., Bonsal, B., and O'Neil, H.: Recent trends in freshwater influx to the Arctic Ocean

3   from four major Arctic-draining rivers, Water, 12(4), 1189, 2020.

4   Amiro, B. D., Todd, J. B., Wotton, B. M., Logan, K. A., Flannigan, M. D., Stocks, B. J., and Hirsch, K. G.: Direct

5   carbon emissions from Canadian forest fires, 1959-1999, Can. J. Forest Res., 31(3), 512-525, 2001.

6   Amiro, B. D., Barr, A. G., Black, T. A., Iwashita, H., Kljun, N., and Mccaughey, J. H.: Carbon, energy and water

7   fluxes at mature and disturbed forest sites, Saskatchewan, Canada, Agric. Forest Meteorol., 136, 2006.

8   Andela, N., Morton, D. C., Giglio, L., Paugam, R., Chen, Y., Hantson, S., and Randerson, J. T.: The Global Fire Atlas

9   of individual fire size, duration, speed, and direction, Earth Syst. Sci. Data, 11(2), 529-552, 2019.

10   Balshi, M. S., et al.: The role of historical fire disturbance in the carbon dynamics of the pan-boreal region: A process-

11   based analysis, J. Geophys. Res., 112, G02029, 2007.

12   Boby, L. A., Schuur, E. A., Mack, M. C., Verbyla, D., and Johnstone, J. F.: Quantifying fire severity, carbon, and

13   nitrogen emissions in Alaska's boreal forest, Ecol. Appl., 20(6), 1633-1647, 2010.

14   Certini, G.: Effects of fire on properties of forest soils: a review, Oecologia, 143, 1-10, 2005.

15   Conard, S. G., and Ivanova, G. A.: Wildfire in Russian boreal forests—Potential impacts of fire regime characteristics

16   on emissions and global carbon balance estimates, Environ. Pollut., 98(3), 305-313, 1997.

17   DeBano, L. F., Neary, D. G., and Ffolliott, P. F.: Fire effects on ecosystems, John Wiley & Sons, 1998.

18   De Groot, W. J., Flannigan, M. D., and Cantin, A. S.: Climate change impacts on future boreal fire regimes, Forest

19   Ecol. and Manage., 294, 35-44, 2013.

20   Denslow, J. S.: Patterns of plant species diversity during succession under different disturbance regimes, Oecologia,

21   46, 18-21, 1980.

22   Ebel, B. A., Moody, J. A., and Martin, D. A.: Hydrologic conditions controlling runoff generation immediately after

23   wildfire, Water Resour. Res., 48(3), 2012.

24   Feng, D., Gleason, C. J., Lin, P., Yang, X., Pan, M., and Ishitsuka, Y.: Recent changes to Arctic river discharge, Nat.

25   Commun., 12(1), 6917, 2021.

26   Franklin, S. B., Robertson, P. A., and Fralish, J. S.: Small-scale fire temperature patterns in upland Quercus

27   communities, J. Appl. Ecol., 613-630, 1997.

28   French, N. H., Kasischke, E. S., and Williams, D. G.: Variability in the emission of carbon‐based trace gases from

29   wildfire in the Alaskan boreal forest, J. Geophys. Res.: Atmos., 107(D1), FFR-7, 2002.

30   Gewehr, S., Drobyshev, I., Berninger, F., and Bergeron, Y.: Soil characteristics mediate the distribution and response

31   of boreal trees to climatic variability, Can. J. Forest Res., 44(5), 487-498, 2014.

32   Gillett, N. P., Weaver, A. J., Zwiers, F. W., and Flannigan, M. D.: Detecting the effect of climate change on Canadian

33   forest fires, Geophys. Res. Lett., 31(18), 2004.

34   Helbig, M., Pappas, C., and Sonnentag, O.: Permafrost thaw and wildfire: Equally important drivers of boreal tree

35   cover changes in the Taiga Plains, Canada, Geophys. Res. Lett., 43(4), 1598-1606, 2016.

36   Hersbach, H., Bell, B., Berrisford, P., Hirahara, S., Horányi, A., Muñoz‐Sabater, J., and Thépaut, J. N.: The ERA5

37   global reanalysis, Q. J. R. Meteorol. Soc., 146(730), 1999-2049, 2020.

Holsinger, L. M., Parks, S. A., Saperstein, L. B., Loehman, R. A., Whitman, E., Barnes, J., and Parisien, M.: Improved Fire Severity Mapping in the North American Boreal Forest Using a Hybrid Composite Method, Remote Sensing in Ecology and Conservation, 8, 222–35, doi:10.1002/rse2.238, 2021.

Iglesias, V., Balch, J. K., and Travis, W. R.: US fires became larger, more frequent, and more widespread in the 2000s, Sci. Adv., 8(11), eabc0020, 2022.

Kasischke, E. S., Hyer, E. J., Novelli, P. C., Bruhwiler, L. P., Nhf, F., and Sukhinin, A. I.: Influences of boreal fire emissions on northern hemisphere atmospheric carbon and carbon monoxide, Glob. Biogeochem. Cycles, 1, 19, 2005.

Kasischke, E.S. and Hoy, E.E.: Controls on carbon consumption during Alaskan wildland fires, Glob. Change Biol., 18, 685-699, 2012.

Kasischke, E. S., and Stocks, B. J. (Eds.): Fire, climate change, and carbon cycling in the boreal forest, Springer Science & Business Media, Vol. 138, 2012.

Kulmala, L., Aaltonen, H., Berninger, F., Kieloaho, A. J., Levula, J., Bäck, J., and Pumpanen, J.: Changes in biogeochemistry and carbon fluxes in a boreal forest after the clear-cutting and partial burning of slash, Agric. Forest Meteorol., 188, 33-44, 2014.

Kurz, W. A., and Apps, M. J.: A 70‐year retrospective analysis of carbon fluxes in the Canadian forest sector, Ecol. Appl., 9(2), 526-547, 1999.

Lamontagne-Hallé, P., McKenzie, J. M., Kurylyk, B. L., and Zipper, S. C.: Changing groundwater discharge dynamics in permafrost regions, Environ. Res. Lett., 13(8), 084017, 2018.

Li, F., Lawrence, D. M., and Bond-Lamberty, B.: Impact of fire on global land surface air temperature and energy budget for the 20th century due to changes within ecosystems, Environ. Res. Lett., 12(4), 044014, 2017.

Liu, W., Fedorov, A., and Sévellec, F.: The mechanisms of the Atlantic meridional overturning circulation slowdown induced by Arctic sea ice decline, J. Climate, 32(4), 977-996, 2019.

McClelland, J. W., Déry, S. J., Peterson, B. J., Holmes, R. M., and Wood, E. F.: A pan‐arctic evaluation of changes in river discharge during the latter half of the 20th century, Geophys. Res. Lett., 33(6), 2006.

McPhee, M. G., Proshutinsky, A., Morison, J. H., Steele, M., and Alkire, M. B.: Rapid change in freshwater content of the Arctic Ocean, Geophys. Res. Lett., 36(10), 2009.

Melillo, J. M., McGuire, A. D., Kicklighter, D. W., Moore, B., Vorosmarty, C. J., and Schloss, A. L.: Global climate change and terrestrial net primary production, Nature, 363(6426), 234-240, 1993.

Moody, J. A., and Martin, D. A.: Initial hydrologic and geomorphic response following a wildfire in the Colorado Front Range, Earth Surf. Process. Landforms, 26(10), 1049-1070, 2001.

Moody, J. A., Martin, D. A., Haire, S. L., and Kinner, D. A.: Linking runoff response to burn severity after a wildfire, Hydrol. Process., 22(13), 2063-2074, 2008.

Moody, J. A., Kinner, D. A., and Úbeda, X.: Linking hydraulic properties of fire-affected soils to infiltration and water repellency, J. Hydrol., 379(3-4), 291-303, 2009.

Moubarak, M., Sistla, S., Potter, S., Natali, S. M., and Rogers, B. M.: Carbon emissions and radiative forcings from tundra wildfires in the Yukon–Kuskokwim River Delta, Alaska, Biogeosciences, 20, 1537–1557, 2023.

1   Mouillot, F., Narasimha, A., Balkanski, Y., Lamarque, J. F., and Field, C. B.: Global carbon emissions from biomass
2   burning in the 20th century, Geophys. Res. Lett., 33(1), 2006.

3   Overeem, I., and Syvitski, J. P.: Shifting discharge peaks in Arctic rivers, 1977–2007, Geografiska Annaler: Ser. A,
4   Phys. Geogr., 92(2), 285-296, 2010.

5   Peterson, B. J., Holmes, R. M., McClelland, J. W., Vorosmarty, C. J., Lammers, R. B., Shiklomanov, A. I., and
6   Rahmstorf, S.: Increasing river discharge to the Arctic Ocean, Science, 298(5601), 2171-2173, 2002.

7   Ponomarev, E., Yakimov, N., Ponomareva, T., Yakubailik, O., and Conard, S. G.: Current trend of carbon emissions
8   from wildfires in Siberia, Atmosphere, 12(5), 559, 2021.

9   Poon, P. K., and Kinoshita, A. M.: Spatial and temporal evapotranspiration trends after wildfire in semi-arid
10   landscapes, J. Hydrol., 559, 71-83, 2018.

11   Rogers, B. M., Soja, A. J., Goulden, M. L., and Randerson, J. T.: Influence of tree species on continental differences
12   in boreal fires and climate feedbacks, Nat. Geosci., 8(3), 228-234, 2015.

13   Rood, S. B., Kaluthota, S., Philipsen, L. J., Rood, N. J., and Zanewich, K. P.: Increasing discharge from the Mackenzie
14   River system to the Arctic Ocean, Hydrol. Process., 31(1), 150-160, 2017.

15   Shakesby, R. A., and Doerr, S. H.: Wildfire as a hydrological and geomorphological agent, Earth-Sci. Rev., 74(3-4),
16   269-307, 2006.

17   Shvidenko, A., Shchepashchenko, D., Sukhinin, A., McCallum, I., and Maksyutov, S.: Carbon emissions from forest
18   fires in boreal Eurasia between 1998-2010.

19   Stuenzi, S. M., Kruse, S., Boike, J., Herzschuh, U., Oehme, A., Pestryakova, L. A., et al.: Thermohydrological impact
20   of forest disturbances on ecosystem-protected permafrost, J. Geophys. Res.: Biogeosci., 127, e2021JG006630, 2022.

21   Sullivan, B. W., Kolb, T. E., Hart, S. C., Kaye, J. P., Hungate, B. A., Dore, S., and Montes-Helu, M.: Wildfire reduces
22   carbon dioxide efflux and increases methane uptake in ponderosa pine forest soils of the southwestern USA,
23   Biogeochemistry, 104, 251-265, 2011.

24   Tan, Z., Tieszen, L. L., and Zhu, Z., et al.: An estimate of carbon emissions from 2004 wildfires across Alaskan Yukon
25   River Basin, Carbon Balance Manage, 2, 12, 2007.

26   Thomas, M. A., Rengers, F. K., Kean, J. W., McGuire, L. A., Staley, D. M., Barnhart, K. R., and Ebel, B. A.:
27   Postwildfire soil‐hydraulic recovery and the persistence of debris flow hazards, J. Geophys. Res.: Earth Surface,
28   126(6), e2021JF006091, 2021.

29   Turetsky, M. R., Kane, E. S., Harden, J. W., Ottmar, R. D., Manies, K. L., Hoy, E., and Kasischke, E. S.: Recent
30   acceleration of biomass burning and carbon losses in Alaskan forests and peatlands, Nat. Geosci., 4(1), 27-31, 2011.

31   Turquety, S., Logan, J. A., Jacob, D. J., Hudman, R. C., Leung, F. Y., Heald, C. L., ... and Sachse, G. W.: Inventory
32   of boreal fire emissions for North America in 2004: Importance of peat burning and pyroconvective injection, J.
33   Geophys. Res.: Atmos., 112(D12), 2007.

34   van der Werf, G. R., Randerson, J. T., Giglio, L., Collatz, G. J., Kasibhatla, P. S., and Arellano Jr, A. F.: Interannual
35   variability in global biomass burning emissions from 1997 to 2004, Atmos. Chem. Phys., 6(11), 3423-3441, 2006.

1 Van Eck, C. M., Nunes, J. P., Vieira, D. C., Keesstra, S., and Keizer, J. J.: Physically‐Based modelling of the post‐
2 fire runoff response of a forest catchment in central Portugal: using field versus remote sensing based estimates of
3 vegetation recovery, Land Degrad. Dev., 27(5), 1535-1544, 2016.

4 Walker, X. J., Rogers, B. M., Baltzer, J. L., Cumming, S. G., Day, N. J., Goetz, S. J., ... and Mack, M. C.: Cross‐
5 scale controls on carbon emissions from boreal forest megafires, Global Change Biol., 24(9), 4251-4265, 2018.

6 Wang, P., Huang, Q., Pozdniakov, S. P., Liu, S., Ma, N., Wang, T., ... and Liu, C.: Potential role of permafrost thaw
7 on increasing Siberian river discharge, Environ. Res. Lett., 16(3), 034046, 2021.

8 Xu, Y., and Zhuang, Q.: The importance of interactions between snow, permafrost and vegetation dynamics in
9 affecting terrestrial carbon balance in circumpolar regions, Environ. Res. Lett., 18(4), 044007, 2023.

10 Xu, Y., Zhuang, Q., Zhao, B., Billmire, M., Cook, C., Graham, J., French, N. HF., and Prinn, R.: Impacts of wildfires
11 on boreal forest ecosystem carbon dynamics from 1986 to 2020, Environ. Res. Lett., under review, 2024.

12 Yin, Y., Bloom, A. A., Worden, J., Saatchi, S., Yang, Y., Williams, M., ... and Schimel, D.: Fire decline in dry tropical
13 ecosystems enhances decadal land carbon sink, Nat. Commun., 11(1), 1900, 2020.

14 Yue, C., Ciais, P., Zhu, D., Wang, T., Peng, S. S., and Piao, S. L.: How have past fire disturbances contributed to the
15 current carbon balance of boreal ecosystems?, Biogeosciences, 13(3), 675-690, 2016.

16 Zhao, B., Zhuang, Q., Shurpali, N., Köster, K., Berninger, F., and Pumpanen, J.: North American boreal forests are a
17 large carbon source due to wildfires from 1986 to 2016, Sci. Rep., 11(1), 7723, 2021.

18 Zheng, B., Ciais, P., Chevallier, F., Yang, H., Canadell, J. G., Chen, Y., ... and Zhang, Q.: Record-high CO_2 emissions
19 from boreal fires in 2021, Science, 379(6635), 912-917, 2023.

20 Zhuang, Q., Mcguire, A. D., O'Neill, K. P., Harden, J. W., Romanovsky, V. E., and Yarie, J.: Modeling soil thermal
21 and carbon dynamics of a fire chronosequence in interior alaska, J. Geophys. Res.: Atmos., 107(D1), 2002.

22 Zhuang, Q. and Xu, Y.: Quantifying the impacts of wildfires on soil thermal, hydrological and carbon dynamics in
23 northern Eurasia from 2003 to 2016, doi: 10.4231/ZJM7-A207,2024
24